A Review of Modeling, Design and Performance Assessment of Linear Electromagnetic Motors for High-Speed Transportation Systems

Lucien Pierrejean, *Graduate Student Member, IEEE*, Simone Rametti, *Graduate Student Member, IEEE*, André Hodder, *Senior Member, IEEE* and Mario Paolone, *Fellow Member, IEEE*

***Abstract*—Linear electromagnetic motors (LEMs) have been proposed, developed and used to propel high-speed (i.e. speed $>$ 100 m/s) levitating vehicles. However, few real implementations have demonstrated the feasibility of these machines at such speeds. Furthermore, LEMs are expected to be enabling technologies for levitating vehicles traveling at near sonic speed, such as the Hyperloop concept. This paper presents a systematic review of modeling, design and performance assessment of LEMs used (or proposed) for the propulsion of levitating high-speed vehicles. Among all the possibilities, those that have received the most attention since the 1960s, along with the first magnetic levitation train concepts, are discussed. Classified by operating principle and topology, the LEMs are compared in terms of design and performance via specific key performance indicators. The performance of the various proposed LEMs is assessed on the basis of data available in the literature.**

***Index Terms*—Transportation, high-speed train, linear electromagnetic motor, electromagnetic propulsion, electromagnetic levitation, maglev.**

I. Introduction

Due to high-dependency on fossil-fuels [1], global transports still accounts for more than 20% of worldwide CO_2 emissions [2], [3]. To meet the greenhouse gas emission targets set by international effort, such as the Paris agreements [4], tomorrow's transports must be more efficient, sustainable, safe and reliable. Electrification of transport, in particular with electric vehicles for low-speed and short-distance travels, is part of this trend [5]. For extended distances, such as intra-continental travel, electric trains, and particularly high-speed trains, are expected to play a larger role in passenger and goods transport. They present low values of average energy usage per passenger per km and CO_2 emissions per passenger per km (e.g. 180 Wh/passenger/km, 20 gCO_2/passenger/km) compared to other transportation systems [6].

The beginning of the 20th century has seen the first electrification of rail transport, previously driven by steam engines, accompanied by constant increase of cruising speed [7]. Then, the conventional wheel-on-rail trains have constantly evolved to achieve high performance and speed, pushing forward the physical limits imposed by wheel-to-rail or pantograph-to-catenary contacts. However, infrastructure constraints, and growth of air transport, finally overtook high-speed train developments. When considering trains currently in service globally, it appears that the highest operating speed is in the order of 80-100 m/s [8], [9]. At the same time, since it was first conceptualised in the early 1900s [10], the magnetic levitation train (i.e., the maglev) has garnered increasing interest since the 1960s due to its feature of operating without any mechanical contact with the guidance infrastructure [11]. More recently, the Hyperloop has attracted the attention in view of its potential cruising speed well higher than the one of a maglev along with its reduced energy needs and passive rail thanks to energy autonomous capsules [6]. Consequently, it has emerged as a promising solution for achieving speeds well beyond those of conventional trains, with targets exceeding 110 m/s [12]. In view of the above, in what follows the term high-speed is used for operating speeds above this value. A comparison of today's speeds for the two types of trains is shown in Table I.

TABLE I
Maximum and commercial speed for two types of HSGT.

	Wheel-on-Rail	Maglev
Speed record	159.4 m/s (TGV)	167.5 m/s (L0 series)
Commercial speed	97 m/s (CR Hexie)	119 m/s (Shanghai Transrapid)

Over time, different machines converting energy into linear motion have been proposed (e.g., rocket, ducted fan, etc.) to propel a maglev train. More recently, the focus has been on linear electromagnetic motors (LEMs) for several reasons [10], [12], [13]:

- high conversion efficiency of electrical power into linear motion through magnetic field;
- contact-free propulsion, independent of any mechanical adhesion factor;
- a single device can create thrust and levitation, increasing the force densities (e.g. volumetric and gravimetric) of the LEM;
- high acceleration and braking force;
- operation in a vacuum environment, without gas emissions;
- low noise emissions;
- expected low rail and wheelset maintenance.

The use of LEMs for high-speed ground transportation (HSGT) has been extensively studied and tested since the 1960s. Additionally, considering the advantages they offer over wheel-on-rail vehicles, LEMs have also been studied

The authors are with the Swiss Federal Institute of Technology (EPFL), Lausanne, Switzerland (e-mail: lucien.pierrejean@epfl.ch)

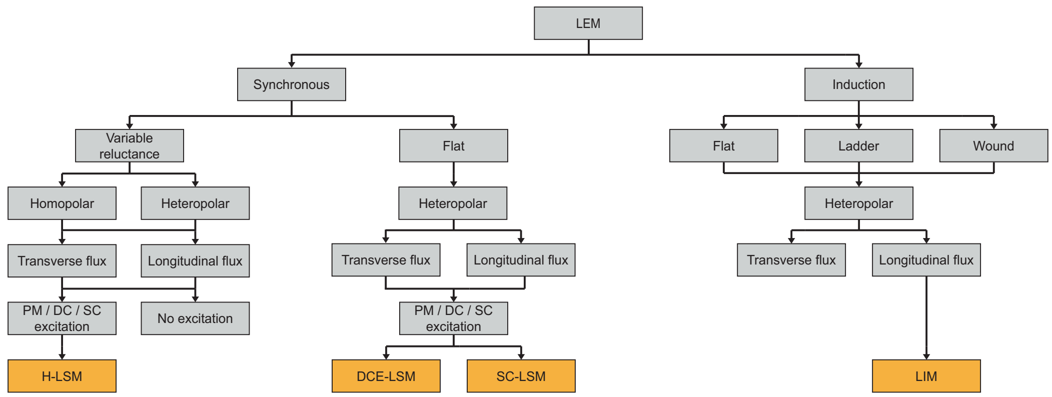

Fig. 1. Classification of LEMs proposed for HSGT propulsion.

and tested to be used in low-speed transport systems such as urban metros [14]. Therefore, not all developed solutions have undergone the same level of testing, and while some have, not all have yet been proven suitable for high speeds.

A limited number of publications have explored the requirements of a high-speed transportation system. The authors of [6] delves into the energy optimization needs, while those of [15] compare the energy consumption. From a different perspective, [16] reviews the core technologies essential to implement a high-speed transportation system.

The main scope of this paper is to review the state of research on LEMs proposed for HSGT propulsion, through their design, modeling and, more specifically, to quantify their performance obtained using data from the literature. These values come from experimental studies on LEMs, obtained from the existing literature, with the aim of demonstrating their feasibility or assessing their performance for a given application, and, to the best of the authors' knowledge, such an analysis has not been proposed in previous reviews in this field [12], [14], [17].

The paper is structured as follows: Section II gives generalities about the use of LEMs in HSGT and extract the main types that are discussed in this paper. Then, Section III and IV describes them in terms of design, modeling, and, particularly, feasibility. They are grouped in these two sections according to their operating principle and topology. Lastly, Section V compare their performance using defined indicators and discuss their improvement margin.

II. LEMs GENERALITIES

So far, several books have summarised the state of research including modeling, design methodology, industrial applications, control strategies and power supply [18]–[24].

Among all the variants proposed for the propulsion of HGST system, LEMs can be classified into 4 categories, as identified in Fig. 1, according to their operating principle and topology:

1) linear induction motor (LIM);
2) DC-excited linear synchronous motor (DCE-LSM);
3) homopolar linear synchronous motor (H-LSM);
4) superconducting magnet linear synchronous motor (SC-LSM).

Variations are also possible, such as the absence of excitation or the addition of permanent magnet (PM) materials. These variations belong to some of the categories mentioned and are addressed at the same time in this paper.

Table II reports the main features of each of these LEMs. These characteristics are discussed in this Section. To assess their performance, specific key performance indicators (KPIs) are introduced. They are used to compare the LEMs and assess the margin improvement of each type. Based on this table, observations specific to the use of LEMs for HSGT propulsion are made.

A. Key performance indicators for LEMs comparison

Although, in terms of operating principle, a LEM using a passive guideway is similar to one using an active guideway, the targeted application and the performance evaluation may be different. Thus, there are two different sets of KPIs, depending on the type of guideway (defined later). For a passive guideway, it is assumed that the necessary energy is provided by an onboard vehicle energy storage systems. It therefore makes sense to scale the performance values to the weight of the motor, given that weight is a major constraint in this type of system.

- The thrust force gravimetric density F_t (p.u.). This is the thrust generated by the LEM, expressed in Newtons (N) and divided by the LEM weight in N.
- If applicable, the levitation force gravimetric density F_n (p.u.). This is the levitation force generated by the LEM, expressed in N and divided by the LEM weight in N.
- The mechanical power gravimetric density P_m (kW/kg). This is the thrust generated by the LEM, multiplied by the speed in m/s and divided by the LEM mass in kg.
- The efficiency-power factor product $\eta \cos \phi$ (p.u.).
- The maximum mechanical speed v_m (m/s).

An active guideway system is characterized by its energy consumption and energy conversion performance.

- The efficiency-power factor product $\eta \cos \phi$ (p.u.).
- The specific energy consumption SEC (Wh/seat/km), assuming fully loaded vehicle, so that one seat equals one passenger. It indicates the minimum energy required to propel a passenger at a given speed per kilometer.

TABLE II
COMPARISON OF LEMS PERFORMANCE AND STRUCTURE.

	LIM	DCE-LSM	H-LSM	SC-LSM
Guideway	Passive	Active	Passive	Active
Topology	Single-sided	Single-sided	Single-sided	Single-sided
Structure complexity	Flat secondary with conductive and magnetic material	Iron-cored, DC excitation on the vehicle	Segmented rail with magnetic material	Core-less, SC magnets on the vehicle
Levitation	EDS/EMS	EMS	EMS	EDS
Flux direction	Longitudinal	Longitudinal	Transverse	Longitudinal
Ratio F_n/F_t [a]	0.5-2	N/S	5-10	N/S
Longitudinal end effect [b]	High	No	Low	No
Magnetic air gap [c]	20-50 mm	10-20 mm	10-20 mm	100-300 mm
Achieved speed	111 m/s	139 m/s	111 m/s	167 m/s

N/S for not specified.
[a] F_t for propulsion force and F_n for levitation force.
[b] Specific effect due to finite length of primary or armature winding.
[c] Core-to-core air gap.

- The maximum mechanical speed v_m (m/s).

A more in-depth discussion of these KPIs and their meaning is presented in Section V-A.

B. Guideway

A LEM can be considered as the cut and unrolled counterpart of a rotary motor and, therefore, consists of two parts. In a transportation application, one component, known as guideway or rail, extends over the entire distance to be covered. Meanwhile, the other component, the moving part that is attached to the vehicle, covers only a very small portion of that distance. Two configurations emerge and are defined as follows [18]:

- Active guideway refers to the presence of an excitation or moving field on the guideway.
- Passive guideway is composed exclusively of conductive or ferromagnetic material. In this case, it is common to talk about rail. The vehicle carries all the active parts of the motor (i.e. multi-phase winding and excitation field, if any).

This is illustrated for two types of linear synchronous motors (LSMs) in Fig. 2. Note that it is chosen to refer to active as soon as the guideway contains excitation of any kind.

C. Levitation

If any, the levitation force produced by the LEM can be associated to two technologies, based on whether it is attractive or repulsive, which depends on the motor's operating principle [25].

- The electrodynamics suspension (EDS) is defined as the interaction between a moving magnetic field and eddy currents induces in a stationary conductive material. This interaction results in a repulsive force. The associated levitation is inherently stable but not active at low speeds, as the interaction takes place with motion.
- The electromagnetic suspension (EMS) is a magnetic attraction between iron and an electromagnet. This levitation principle is inherently unstable and needs to be controlled with a feedback loop. Indeed, the attraction force is non-linear with the air gap.

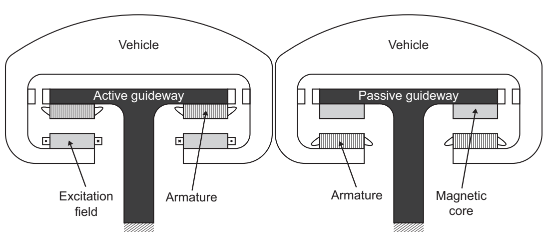

(a) DCE-LSM (b) H-LSM

Fig. 2. Structure of (a) an active guideway and (b) a passive guideway.

D. Air gap

The air gap in electrical motors is determined by the motor's structure, speed, and application requirements. Unlike rotary motors with air gaps of typically 0.2-3 mm [26], the performance of LEMs is often influenced by the presence of larger air gaps of several centimeters required for HSGT applications.

At high speed, a precise control of the air gap is essential to avoid any contact with the guideway and to handle disturbances such as train crossings or crosswinds. For passenger comfort, a small air gap reduces flexibility for smooth levitation control, which may require additional mechanical damping between the motor and the passenger cabin and a higher instantaneous power required at inverter's output [27].

E. Design aspects

1) Definitions

While there are similarities between rotary and linear electromagnetic motors, LEMs offer additional degrees of freedom. In particular, they can be designed as single-sided or double-sided motors, providing enhanced flexibility in the motor assembly. In a double-sided configuration, the magnetic flux is crossing the air gap from one side to the other. This is illustrated in Fig. 3 for a linear induction motor (LIM), where the two primary parts are located on both side of a

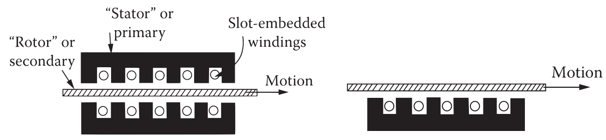

(a) DSLIM (b) SLIM

Fig. 3. Double-sided and single-sided LIMs. Adapted from [18].

central rail. In this case, normal forces on two primary parts counterbalance each other.

Additionally, the motor can be either longitudinal or transverse flux as illustrated in Fig. 4. This term relates to the direction of the magnetic flux: in a longitudinal flux motor, the magnetic field is flowing in the direction of the motor's motion, while in a transverse flux motor, it flows within a plane perpendicular to the motion direction. A transverse flux motor is preferred when the magnetic path of the transverse configuration is shorter than that of the longitudinal configuration. This reduces the iron thickness iron and, therefore, the total motor weight [28]–[30]. A transverse flux machine usually has a higher force density, a high efficiency, but a low power factor and a complex structure, making it more difficult to model [31].

Among LEMs, the term *homopolar* or *heteropolar* defines the polarity in the air gap, i.e the sign of the magnetic field. In a homopolar machine, the polarity over the entire surface of a single air gap is constant [32]. As shown in Fig. 4b or 8a, these are typically transverse flux machines, and a single air gap corresponds to one side of the U-shaped primary or armature.

2) Design optimization

A design optimization process requires fast and accurate models that assess the motor performance. Generally, the focus is on developing analytical models that take into account few or all effects and give acceptable results in a short time. Models using finite element method (FEM) represent a powerful alternative to analytical models. However, when three-dimensional analysis are needed, it requires considerable computational resources [33]. The optimization procedure is divided into several sequential steps [34]. Firstly, a single- or multi-objective function with variables to minimize or maximize is proposed. Following this, key constraints are identified and defined, outlining permissible intervals for the design parameters. These key constraints may be complemented by design guidelines, offering opportunities to enhance the design without being mandatory. Finally, a specific solving method is employed, followed by an analysis of the obtained results.

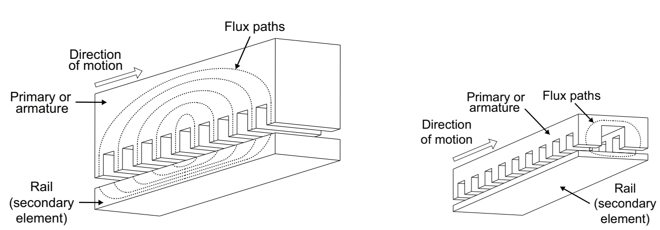

(a) (b)

Fig. 4. Illustration of (a) longitudinal and (b) transverse flux.

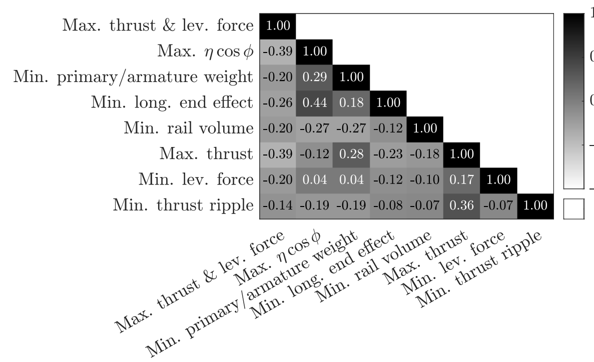

(a) Correlation matrix of objective function variable

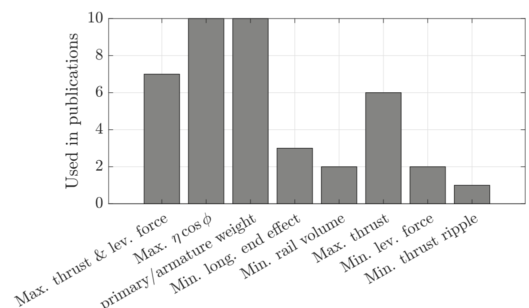

(b) Occurrence of objective function variables in publications

Fig. 5. Analysis of objective function variables used in LEM design optimization.

Fig. 5b represents the occurrence of variables within objective functions as they appear in a sample of the literature on LEM design optimization [35]–[52]. Fig. 5a shows the correlation matrix of the variables, i.e. the likelihood that two variable are maximised / minimised in the same design procedure.

Although some studies aim to minimize the levitation force, the main objective in the design optimization of LEM is to maximize the force gravimetric densities created by the motor (especially the thrust) and the efficiency-power factor product. These design procedures also include some specific effects related to the type of LEM. Indeed, for a LIM, the impact of the longitudinal end effect is likely to be minimized and the efficiency-power factor product maximized, whereas for some LSMs the aim is to minimize thrust ripple for maximum thrust.

However, in LEM design studies, it is important to investigate the other significant characteristics to ensure the operational feasibility of the system. These include analyzing the vibrations created by the motor, assessing the fault tolerance and making the system safer, predicting heating and its impact on the performance, etc.

F. Performance impact on power supply

Efficiency and power factor are important performance indicators for LEMs, as they determine the size of the power electronics and have a direct influence on the energy consumption of the transportation system [44].

An advantage of LEMs is their ability to do active braking, and braking energy can be fed back into the main supply.

The transfer of energy from the infrastructure to the vehicle, when the latter has no energy storage system, can take place via a mechanical contact between the two, for example a pantograph-to-catenary contact. However, mechanical contact is undesirable at high speeds, making inductive power transfer the most suitable solution [53]. Alternatively, the energy needed to operate the vehicle has to be stored onboard.

III. Linear induction motor

The LIM operates based on the principle of electromagnetic induction. The primary part, containing the winding, induces currents in a secondary element, generating thrust through the interaction between the magnetic field generated by the primary winding and the induced currents in the secondary element.

A. *Design aspects*

The operating principle of a LIM is similar to the rotary induction machine (IM), allowing several secondary types [54], [55]. Since the performance of a LSM is better than that of a LIM for an active guideway, the latter is of interest when used with a passive guideway [18], [33]. Indeed, a secondary made of a conductive sheet alone or combined with layers of magnetic material are commonly considered due to their ease of manufacturing and assembly over long distances, as illustrated in Figure 6b .

In a double-sided LIM (DSLIM), the two primaries are located on either side of a central rail, as shown in Fig. 3a, cancelling the normal force exerted by the primary assembly on the rail. In a single-sided LIM (SLIM), the normal force (or levitation force) can be repulsive (EDS) or attractive (EMS), depending on the secondary used and the operating point of the motor [58]–[62]. Several studies have focused on rail characteristics, material properties and general design. The presence of secondary joints affect the vehicle dynamics [63], whereas design and material variations can improve SLIM performances [54], [61], [64]–[66]. The thermal behavior of this type of motor is analysed, for instance, in [46], since a passive guideway implies the primary to be continuously supplied during the ride.

LIMs, and especially DSLIMs, have a large air gap, due to the required clearance imposed by the speed and the conductive rail, magnetically seen as air [14]. A larger air gap implies a higher magnetising current and, therefore, reduces the machine's power factor and efficiency [44], [67].

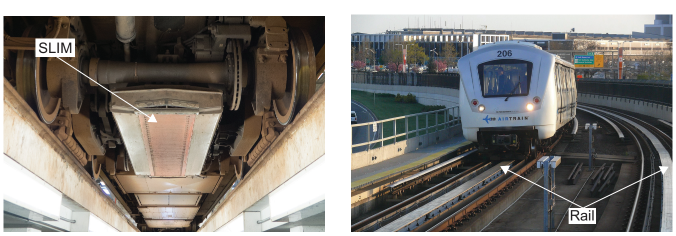

(a) Primary (SkyTrain) (b) Secondary (JFK AirTrain)

Fig. 6. SLIM as a propulsion system for a wheel-on-rail train. Adapted from [56], [57].

B. *Modeling*

1) *End effects*

Specific phenomena caused by the finite lengths of the primary are called end effects [64]. The transverse end effect occurs in the direction perpendicular to the motion, while the longitudinal end effect is caused by the relative motion between the primary and the secondary. As a result, they decrease the thrust, lift, efficiency and power factor [33], [68].

Although the causes and consequences of these effects are widely documented in the literature, their accurate modeling is still being investigated at the present time. It is often proposed to reduce these negative effects at the design stage, as proposed by Laithwaite with the goodness factor [22] aiming to design a LIM that is least affected by the longitudinal end effect at its operating point, or by others with the end effect factor [47], [69], [70]. However, studies have proposed to use it to improve LIM performance [71]. Overall, the literature agrees that a high number of poles reduces the impact of the longitudinal end effect [69].

2) *Analytical models*

During the 1970s, the focus was on understanding the end effects and modeling the LIMs with advanced analytical models such as one-, two-, three-dimensional field-based models[1] [62], [65], [72]. In recent years, the main effort is directed to the development of equivalent circuit models (ECM) that accurately account for the longitudinal end effect, air gap variations and magnetic saturation [47], [73]–[75]. This need is mainly associated to the coupling with the control of the motor's power electronics [14], [76]. The main innovation is the extensive use of FEM (two or three-dimensions) which provides accurate results since the numerical solution is obtained with no approximation of the underlying physics [46]–[48], [64], [68], [77]. The limitation is the computation time, which limits its use to model validation or specific analysis [78].

Table III gives a comparative analysis of LIM models, providing key assumptions, captured effects, limitations and advantages. Field-based two- and three-dimensional models provide fast and relatively accurate results, which can be used in design optimization algorithms. Carter's coefficient has been widely adopted in the literature to take primary slots into account [79]. It defines an equivalent air gap length, used in the model equations, so the primary surface can be considered to be flat [18], [26]. The assumption of constant iron permeability implies that there is no saturation accounted for, especially in the primary or in the back-iron. The use of steady-state conditions allows to derive the model in the frequency domain and to use phasors. Finally, assuming a constant rail conductivity means neglecting frequency-related effects. These assumptions greatly simplifies the formulation of the model along with improving computational effectiveness.

C. *Performance impact on control*

The end effects have an impact on the LIM control scheme and make it more complicated to implement [14], [33]. In the

[1]A field-based model solves the governing differential equations using methods such as the Fourier series decomposition.

TABLE III
COMPARATIVE ANALYSIS OF LIM MODELS.

Model dimension	1D	2D	3D
Model type	ECM [42], [47], [73]–[75], [80]	FEM [46]–[48] Field-based [62], [65], [72], [81]	FEM [48], [64], [68], [77], [82] Field-based [83]
Geometry representation	None	Longitudinal plane	Full
Primary slots	None	Carter's coefficient	Fully considered or Carter's coefficient
Longitudinal end effect	Often neglected [a]	Often considered	Considered
Transverse end effect	Often neglected [a]	Often neglected [a]	Considered
Main assumptions	Constant iron permeability, constant rail conductivity, steady-state conditions		
Computation time	Low	High	Analytical: high FEM: very high
Application	Motor control Performance estimation	Design Performance estimation	
Advantages	Low complexity	High accuracy	
Limitations	Limited accuracy	No edge effect	High complexity

1D, 2D, 3D for one, two, three dimensions.
ECM for equivalent circuit model, which can be magnetic or electrical.
[a] This effect is sometimes considered using specific coefficients.

absence of the latter, the theory of transients, as developed for rotary IM, may be used [84].

LIMs are supplied by a variable-frequency source, so that they are set to a precise operating point for each speed, such as the maximum efficiency-power factor product, which is usually located at higher slip than in rotary IM, due to the higher air gap [59], [65], [68], [85].

D. Feasibility

By far the most extensively tested LEM is the LIM, some of which have reached 111 m/s [86], and which has been used in commercial transport applications. However, the longitudinal end effect, and its poor performance at high speed, seems to have limited its use to low-speed applications, such as Linimo (28 m/s) in Nagoya [87], SkyTrain in Vancouver or AirTrain in New York [10]. The first mentioned uses a EMS device for the levitation and the last two are not maglev trains but wheel-on-rail LIM-powered trains. Even though they are SLIMs, the normal force generated is not used to levitate the vehicle.

IV. Linear synchronous motor

The LSM is characterised by the synchronism of the mechanical motion with the moving magnetic field [19]. Thrust is created by the interaction between the moving magnetic field and a variable reluctance structure, or a magnetic excitation field.

A. Design aspects

1) DC excitation with active guideway

The DC-excited LSM (DCE-LSM) is a LEM with an active guideway, in which the AC armature winding is usually set on the guideway and the DC excitation winding (named exciter) on the vehicle, both iron-cored [18], [88]. The exciter is also used for the levitation of the vehicle (EMS). An additional winding can be housed in the exciter teeth as shown in Fig. 7a, it is a linear transformer used to transfer energy from the guideway to the vehicle. Possible design variations of the motor are the flux direction or winding layout [89].

2) DC excitation with passive guideway

The active guideway is a complex solution to be used for long distances. A proposed alternative is to move the excitation winding to the armature, and the armature to the vehicle, so that all windings are located on the same side of the motor, and the motor on the vehicle. In this case, the rail is passive and made of a segmented ferromagnetic structure notched along the direction of motion. Several motor design can be considered: heteropolar or homopolar, transverse or longitudinal flux [32]. Nevertheless, the solution that emerges to simplify manufacturing is the transverse flux homopolar LSM (H-LSM), shown in Fig. 8a. Naturally, the same motor could be used in an active guideway application and a passive vehicle, as was the case for the Swissmetro concept [92].

The H-LSM design is very flexible and the rail shape can be optimized to modify motor's performance such as cogging thrust or ratio of levitation force to propulsion force [94], [95]. Fig. 9 illustrates this flexibility with two different rail shapes.

A drawback of the H-LSM is the high flux density experienced by the armature teeth. The other notable downside is the large space occupied by the coils in the armature [96]. Indeed, a large part of the coil is not located under the armature active surface. The complex shape of the latter leads to a bulky and heavy motor, with a small active surface, which is an issue

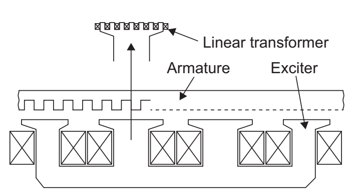

(a) DCE-LSM with linear transformer

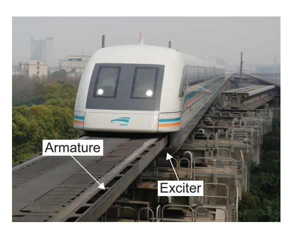

(b) Shanghai Transrapid

Fig. 7. Active guideway with DCE-LSM and the Shanghai Transrapid. Adapted from [90], [91].

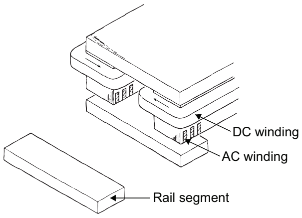

(a) H-LSM

(b) Magnibus

Fig. 8. Passive guideway with H-LSM and the Magnibus. Adapted from [29], [93].

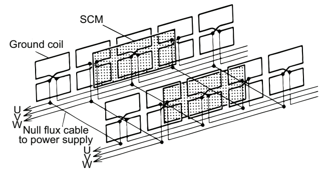

(a) Core-less SC-LSM with eight-shaped coils

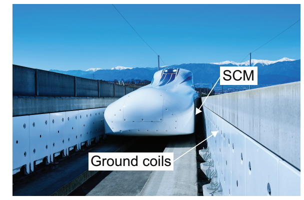

(b) L0 series train

Fig. 10. Active guideway with SC-LSM and L0 series at Yamanashi test line. Adapted from [103], [104].

for applications with on-board energy storage system. In this case, the focus is on designing a armature that is optimized in terms of weight and volume. Briefly mentioned in the literature for transport application, the reluctance LSM is equivalent to the H-LSM without the DC excitation, in a longitudinal flux configuration [97]–[99].

Additionally, PMs can be added to the exciter of DC excited LSM [19], [97], [100], [101] or in the armature of the H-LSM [18], [102] in order to reduce the size of the DC winding. The PMs ensure the levitation of the total vehicle weight and the DC coils are used only for controlling the levitation stability. This results in configurations with high gravimetric and volumetric densities for thrust.

In this case, the same considerations apply as for PM rotating synchronous machines (PM-SM), and irreversible demagnetization of the magnets due to the magnetic field created by the windings may occur. The maximum allowed temperature of the exciter is also limited. Indeed, it is usually kept below 100-150 °C to avoid degradation of PMs performance [99].

3) SC excitation

For large-power and high-speed LSMs, the exciter with ferromagnetic core that create the excitation flux in the DCE-LSM can be substituted by superconducting electromagnets (SCM) [19]. The goal is to keep a core-less coil at extremely low temperature, namely 10K or 77K for high-temperature superconductive (HTS) materials, so that a large current can flow in it with negligible Joule losses. In this case, it is possible to obtain a high magnetic flux density in the air gap. Once a DC current is flowing in the coil, it may stay for several hours [19]. The input power required for cooling is lower with HTS and all the complexity lies in the design and the operation of the SCM [18].

SC-LSM usually have SCM on the vehicle and a core-less AC armature winding on the guideway [18], [88]. The AC winding is placed horizontally, as shown in Fig. 11, or vertically (laterally on the two sides), as shown in Fig. 10a. The latter configuration, seems to provide better force density and allows to have propulsion, levitation (EDS) and guidance with a low magnetic drag [106].

The SC-LSM stands out for its high-permissible clearance between the vehicle and the guideway, with mechanical air gap of at least 5-10 cm and magnetic of 30 cm (core-to-core) [106], [107].

B. Modeling

Similarly to the LIM, there exists a longitudinal end effect for H-LSM. Each rail segment entering or leaving the flux created by the armature experiences a flux variation and, as a result, eddy currents are induced in it, thereby producing a drag force [108]. A drag force is also present in the DCE-LSM, due to the levitation and guidance electromagnets moving over an iron-cored rail. However, the resistivity of the iron is high and it is expected that the induced currents decay rapidly [29], [109], [110]. At the cost of complexity, it is also possible to use a laminated rail [108]. Analytical determination of eddy current generation in these LEMs is not trivial, as they are made up of a doubly-salient structure [29], [110]–[113]. The main challenge in designing lies in estimating the flux path, specifically the permeance in the air gap between two opposing structures and, consequently, in developing an accurate model of iron saturation [31].

Due to its inherent levitation principle involving the generation of eddy currents in passive conductors, the SC-LSM introduces a magnetic drag force that varies based on the type of guideway. In the configuration depicted in Fig. 10a, the drag force results from eddy currents induced in the eight-shaped coils, which concurrently contribute to the levitation force. In

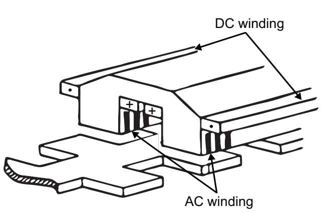

(a) Alternating rail segment

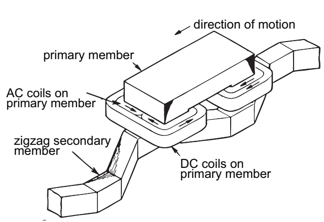

(b) Zig-zag rail

Fig. 9. Different rail geometries for H-LSM. Adapted from [17].

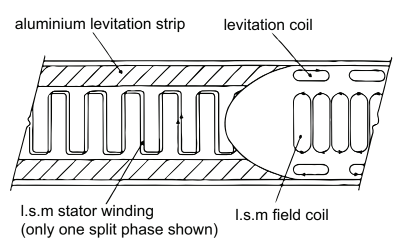

Fig. 11. Active guideway with SC-LSM and horizontal armature winding. Adapted from [105].

TABLE IV
LSM MODELING COMPARISON.

	H-LSM	DCE-LSM	SC-LSM
Model type	ECM [95] Field-based [18], [110] Permeance and MMF [114], [118]–[120] FEM [118], [129], [130]	ECM [131], [132] Field-based [18], [78], [133] FEM [89], [117], [134]	ECM [106], [135] Field-based [52], [115], [116], [136] FEM [106], [107], [115], [116], [136]
Geometry representation	Full [a]	Longitudinal plane or full	Full [b]
Armature slots	Often considered	Considered or Carter's coefficient	N/A
Drag force	Often neglected	Often neglected	Often neglected
Main assumptions	Constant iron permeability No eddy currents Permeance function often simplified Steady-state conditions	Constant iron permeability No eddy currents Steady-state conditions	Simplified model of air gap MMF Constant magnetic field created by SCM

N/A for not applicable.
[a] Imposed by the nature of the H-LSM which is a transverse flux machine.
[b] Most studies consider propulsion, levitation and guidance forces.

the modeling of the SC-LSM illustrated Fig. 10a, the drag force is often neglected because of its relatively low impact compared to the aerodynamic drag in these open-air HSGT systems.

Often, modeling involves determining the air gap flux density using magnetomotive force (MMF) [114]–[120], although various approaches exist. Table IV presents a comparative analysis of LSM modeling methods, outlining the key assumptions or effects considered in the models. Simplifying the model by neglecting eddy currents, implies that no drag force and/or core losses are considered. A simplified model of the permeance function, or air gap MMF, is equivalent to neglecting certain effects on the flux, such as fringing or leakage, complex to model in variable-reluctance structures [121]–[123]. It appears that the literature on DCE-LSM modeling benefits from that on PM-LSM, which is very comprehensive, since the motor structure and operating principle are similar, with the only distinction being the excitation field source [124]–[128]. However, PM-LSMs are mainly used in automation applications with low energy consumption and short travel distances [78].

C. Impact of active guideway on performance

An active guideway is supplied by several substations over the entire distance to be covered. The segment between two substations is divided into sections about a kilometer long, depending on the environment, which are energised when the vehicle is moving inside [17]. The power factor and efficiency of active guideway LSMs is related to the length of the energised section [115], [137]. The length and characteristics of the section depend on the vehicle dynamics at that location.

D. Propulsion and levitation control flexibility

Propulsion and levitation control can be decoupled: the levitation being controlled by the onboard DC winding while the propulsion through externally supplied ground stations [93], [138]. The thrust can be varied only by the magnitude and the phase angle of the armature current [18], [19], [139].

A major advantage of LSMs with excitation is the ability to adjust the power factor by controlling the DC field current, resulting in LEMs with high power factors [78], [119], [140], [141].

E. Feasibility

So far, in 1988 a prototype using a H-LSM has been built and tested for a urban transit application [93], [142]. A configuration with an armature set on the infrastructure and a rail on the vehicle was chosen for the propulsion of Swissmetro in the 90's [143]. Despite this, it has never been used in commercial applications. DCE-LSM with active guideway is the propulsion used for the Transrapid, whose commercial application is the Shanghai Transrapid. For the time being, the SC-LSM is the solution retained for world fastest trains (167.5 m/s), the Shinkansen L0 is currently tested at the Yamanashi test line and an opening to commercial traffic is planned in the years to come.

V. PERFORMANCE ASSESSMENT

A. Systematic review methodology

In order to gather data from the existing literature to assess the performance of LEMs, a systematic search approach has been employed. This search was carried out in the following databases:

- Scopus[2], which includes:
  - IEEE Explore,
  - ScienceDirect,
  - IET,
  - Springer,
  - MDPI,
  - Taylor and Francis,
  - Emerald Insight.
- EPFL Library[3].

Both databases share common publishers while also complementing each other by encompassing areas that are not addressed by the other. Only experimental values from tests reaching speeds greater than 10 m/s, from which the KPIS defined in Section II-A can be calculated or extracted directly, have been selected.

It is not always possible to directly infer the corresponding KPI value from each reference. Either because the value is given for different operating points, then one has to be

[2]https://www.scopus.com
[3]https://epfl.swisscovery.slsp.ch

selected, or because the value is not directly indicated, but can be calculated from what is given. For this purpose, the following summarizes how the values of Table V have been assessed.

- The thrust gravimetric density F_t is taken at its maximum value, at the maximum speed v_m.
- The levitation force gravimetric density F_n is taken at the same operating point as the thrust gravimetric density.
- The mechanical power gravimetric density P_m is given by $P_m = v_m F_t$.
- The efficiency-power factor product $\eta \cos \phi$ is taken at its maximum value, at the maximum speed v_m. Additionally, it can be calculated as the ratio of maximum mechanical power to input apparent power $\eta \cos \phi = mP_m/S$. Where S being the apparent power and m the mass of the LEM. In this case, it is assumed that the maximum mechanical power is obtained with the maximum available apparent power, at the maximum speed.
- The specific energy consumption is taken at the motor output and corresponds to the minimum energy required to overcome the tractive resistance of the vehicle. Thus, at a given speed v_m, for a given number of seats in the vehicle N_{seat}, it can be calculated from the traction power P_{tr} as $SEC = P_{tr}/(N_{\text{seat}} v_m)$.

TABLE V
OVERVIEW OF LEM PERFORMANCE.

	F_t (p.u.)	F_n (p.u.)	P_m (kW/kg)	$\eta \cos \phi$ (p.u.)	SEC (Wh/seat/km)	v_m (m/s)	v_m (km/h)	Reference
LIM	-	-	-	0.38	-	10.2	37	[67]
	1.00	-	0.12	0.42	-	12	43	[17]
	-	-	-	0.33[c]	-	12	43	[144]
	-	-	-	0.40[a]	-	13	47	[145]
	-	-	-	0.25[a]	-	13.9	50	[60]
	0.93	-	-	0.25[c]	-	15	54	[17], [144]
	1.19	-	0.18	0.32	-	15	54	[146]
	1.22	-	0.18	0.43	-	15.3	55	[147]
	0.71[a]	0.51[a]	0.11	-	-	15.7	56	[68]
	-	-	-	0.44[a]	-	15.8	57	[73]
	-	-	-	0.38	-	18.1	65	[148]
	1.42[a]	-	0.35	0.41[a]	-	25	90	[149]
	-	-	-	0.50[c]	-	30.6	110	[144]
	1.86[a]	-	0.63	0.39[a]	-	34.7	125	[149]
	-	-	-	0.22	-	48	173	[150]
	-	-	-	0.30[a]	-	51.4	185	[60]
	0.63[a]	1.40[a]	0.32	0.19[a]	-	52.3	188	[59]
	1.90[a]	-	0.98	0.45[a]	-	52.8	190	[149]
	0.75[a]	0.31[a]	0.43	0.35	-	58.3	210	[59]
	-	-	-	0.23[a]	-	59.5	214	[72]
	-	-	-	0.24[a]	-	69.4	250	[60]
	-	-	-	0.55	-	83.3	300	[151]
	1.30[a]	-	1.07	0.36[a]	-	83.3	300	[149]
	-	-	-	0.13[a]	-	108	389	[86]
H-LSM	0.61	-	0.06	-	-	10	36	[152]
	0.71	4.77	0.08	0.50	-	12	43	[120]
	0.72	-	0.09	0.79	-	12	43	[17]
	0.71	7.14	0.11	0.64	-	15	54	[93]
	-	-	-	0.64[a]	-	27.8	100	[111]
	-	-	-	0.72[a]	-	55.6	200	[111]
	-	-	-	0.78[a]	-	83.3	300	[111]
	-	-	-	0.71[b]	54[b]	103.3	372	[153], [154]
	-	-	-	0.44[a]	-	111.1	400	[113]
	0.60	4.20	0.66	0.41	-	111.7	402	[109]
DCE-LSM	-	-	-	-	22	55.6	200	[13]
	-	-	-	0.76	34.7[b]	68.1	245	[155], [156]
	-	-	-	-	30.6	83.3	300	[144]
	-	-	-	-	34	83.3	300	[13]
	-	-	-	-	48.6	111.1	400	[144]
	-	-	-	0.79[c]	83.3[b]	111.1	400	[27], [155]
	-	-	-	-	52	111.1	400	[13]
	-	-	-	0.77[c]	72.2	138.9	500	[144]
SC-LSM	-	-	-	-	54[b]	83.3	300	[157]
	-	-	-	0.96[c]	-	100	360	[144]
	-	-	-	0.69[c]	-	138.9	500	[144]
	-	-	-	-	99[b]	138.9	500	[157]
	-	-	-	0.63[c]	-	143.6	517	[158]

[a] Estimated based on graphics or images.
[b] Given as estimated value.
[c] Assuming that all installed power is used to generate maximum thrust.

B. Results and discussion

The performance of the above-mentioned LEMs is assessed using data taken from the literature, via the KPIs defined Section II-A. All the values are listed in Table V, organized according to LEM type, from lowest to highest speed, and shown in Figs. 12, 13 and 14.

The first and second columns of Table V show the force gravimetric densities for the LIM and H-LSM in per unit (p.u.). The thrust gravimetric densities show comparable magnitudes, with slightly higher values for the LIM (1÷1.8 for the LIM vs 0.6÷0.8 for the H-LSM). Fig. 12 shows the mechanical power gravimetric densities, where the red line in the box plot represents the medians of the distributions. It appears that the LIM exhibits higher values than the H-LSM and, as this quantity is related to the speed, it means that for the same speed, the LIM produces a higher thrust gravimetric density than the H-LSM. However, the average performance of a rotary SM used to propel conventional wheel-on-rail train (indicated by a dash-dotted line in Fig. 12) provides a quantification of the potential for improvement of H-LSMs. Further experimental validations at high-speeds with optimised motor designs could support this observation.

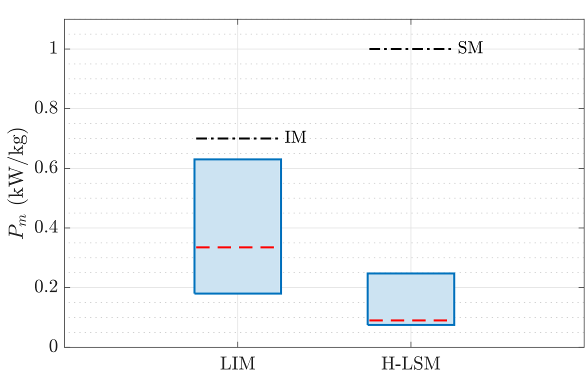

Fig. 12. Distribution of mechanical power gravimetric density for the LIM and H-LSM. The median is represented by the dashed line and the min/max values are given by the first and third quartiles. The dash-dotted line indicates the average performance rating of the rotary equivalent for a conventional wheel-on-rail train, adapted from [8], [84].

Upon further examination of Table V, it is observed that the levitation force gravimetric density of the H-LSM is approximately ten times greater than its thrust gravimetric density (4÷7), whereas these values are smaller for the LIM (0.7÷1.3). Notably, the spread of levitation force gravimetric density is wider for the H-LSM.

The specific energy consumption of the LEMs employed in active guideway solutions is shown in Fig. 13. It is important to emphasize that this representation does not account for the efficiency of the LEMs. If efficiency were considered, the data points in Figure 13 would shift upward, resulting in an increase in specific energy consumption. These values are taken from vehicles travelling in open air, where increasing the speed increases the vehicle's aerodynamic resistance and therefore the energy required to propel it. This trend is consistent across different types of LEMs, as evident on the figure.

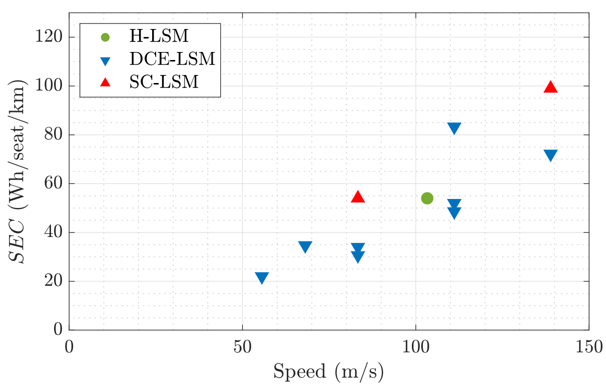

Fig. 13. Comparison of specific energy consumption at different speeds, for the H-LSM, DCE-LSM and SC-LSM.

A major indicator, common to all LEMs, is the efficiency-power factor product, shown in Fig. 14. It illustrates the LEM's energy conversion and the sizing of the power electronics that supply it. Overall, it can be seen that LSMs have better performance than LIM, in the same way that a rotary SM outperforms an IM. Although there are specific effects in LEMs affecting their performance, the margin of improvement compared with the average performance of a rotary equivalent, indicated by a dash-dotted line in Fig. 14, is significant, especially for LIMs. Finally, it is worth noting that the highest values of efficiency-power factor product are obtained with large machines, in terms of power and size, even if they run at high speeds. This is interesting as the same consideration apply for rotary motors [26]. Values of efficiency-power factor product above 0.6 for optimized and high-power LIMs are achievable, as well as values above 0.8 for H-LSMs.

The important point to note when looking at these data is that they are limited and predominantly derived from experiments conducted last century. Moreover, most experimental validations were carried out on small-scale, low-power, low-speed (i.e. < 10 m/s) prototypes. This is especially true for LEMs with passive guideways, whereas those with active guideways are already used in commercial high-speed transportation systems (or will be soon). This underlines the need for further testing of LEMs with passive guideway to validate their potential to propel real scale HSGT systems.

VI. Conclusion

In this paper, a systematic review of modeling, design and performance assessment of LEMs has been proposed. They

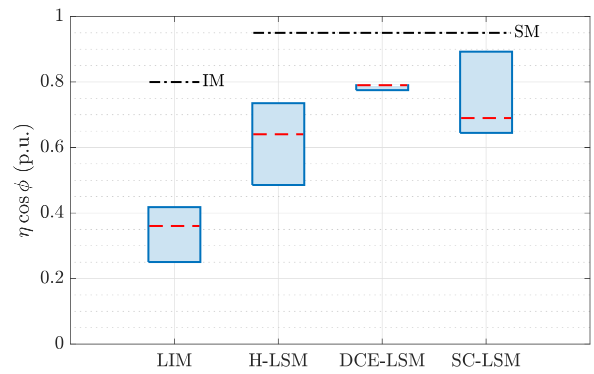

Fig. 14. Comparison of the efficiency-power factor product distribution for the LEMs. The median is represented by the dashed line and the min/max values are given by the first and third quartiles. The dash-dotted line indicates the average performance rating of the rotary equivalent for a conventional wheel-on-rail train, adapted from [8], [84].

are classified into 4 categories, according to their operating principle and topology, which are the LIM, the H-LSM, the DCE-LSM and the SC-LSM.

The LIM is used in a passive guideway application and has the advantage of a very simple rail design. It has been intensively studied and tested in the last decades. Despite poorer performance compared to LSMs, good performance is expected for high-power machines and optimized design, with values of efficiency-power factor product above 0.6 and thrust gravimetric density between 1 and 1.8.

Similarly to the LIM, the H-LSM is used in a passive guideway application, with a better efficiency-power factor product (expected to be above 0.8) at a cost of a more complicated rail design. The thrust gravimetric density is between 0.6 and 0.8. However, additional modeling and high-speed experimental validation are still required.

It appears that no reference has yet carried out a complete study of the LIM and H-LSM, integrating all motor characteristics, with the aim of determining the maximum theoretical limit in terms of performance.

On the other hand, the DCE-LSM and SC-LSM are employed in active guideway applications and exhibit good performance even at high speeds, with efficiency-power factor products above 0.7. Deployment of applications using these LEMs appears to be limited due to the complexity (cost) of the guideway, which requires a power supply along the entire distance. Although the specific energy consumption, estimated around 60 Wh/seat/km at 111 m/s, is competitive regarding other type of transportation, to date, the longest distance covered by a maglev is the 30 km Shanghai Transrapid, which uses a DCE-LSM.

References

[1] IEA. "Energy consumption in transport by fuel in the net zero scenario, 1975-2030." (2022), [Online]. Available: https://www.iea.org/data-and-statistics/charts/energy-consumption-in-transport-by-fuel-in-the-net-zero-scenario-1975-2030.

[2] IEA, "CO2 emissions in 2022," IEA, Paris, 2023, https://www.iea.org/reports/co2-emissions-in-2022.

[3] IEA. "Global CO2 emissions from transport by sub-sector in the net zero scenario, 2000-2030." (2022), [Online]. Available: https://www.iea.org/data-and-statistics/charts/global-co2-emissions-from-transport-by-sub-sector-in-the-net-zero-scenario-2000-2030-2.

[4] UNFCCC. "The paris agreement." (Dec. 2015), [Online]. Available: https://unfccc.int/process-and-meetings/the-paris-agreement.

[5] International Energy Agency, *Global EV Outlook 2023: Catching up with Climate Ambitions* (Global EV Outlook). OECD, Apr. 26, 2023. DOI: 10.1787/cbe724e8-en.

[6] D. Tudor and M. Paolone, "Optimal design of the propulsion system of a hyperloop capsule," *IEEE Transactions on Transportation Electrification*, vol. 5, no. 4, pp. 1406–1418, Dec. 2019. DOI: 10.1109/TTE.2019.2952075.

[7] D. Hasegawa, G. L. Nicholson, C. Roberts, and F. Schmid, "Standardised approach to energy consumption calculations for high-speed rail," *IET Electrical Systems in Transportation*, vol. 6, no. 3, pp. 179–189, 2016. DOI: 10.1049/iet-est.2015.0002.

[8] S. Paul, P.-W. Han, J. Chang, Y.-D. Chun, and J.-G. Lee, "State-of-the-art review of railway traction motors for distributed traction considering south korean high-speed railway," *Energy Reports*, vol. 8, pp. 14 623–14 642, Nov. 2022. DOI: 10.1016/j.egyr.2022.10.411.

[9] P. Nilson. "The 10 fastest high-speed trains in the world," Railway Technology. (Jun. 5, 2023), [Online]. Available: https://www.railway-technology.com/features/the-10-fastest-high-speed-trains-in-the-world/.

[10] R. Hellinger and P. Mnich, "Linear motor-powered transportation: History, present status, and future outlook," *Proceedings of the IEEE*, vol. 97, no. 11, pp. 1892–1900, Nov. 2009. DOI: 10.1109/JPROC.2009.2030249.

[11] E. R. Laithwaite, Ed., *Transport without wheels*, London: Paul Elek, 1977, 322 pp.

[12] H.-W. Lee, K.-C. Kim, and J. Lee, "Review of maglev train technologies," *IEEE Transactions on Magnetics*, vol. 42, no. 7, pp. 1917–1925, Jul. 2006. DOI: 10.1109/TMAG.2006.875842.

[13] T. International, "High-tech for flying on the ground," Berlin, Germany, Brochure, May 2002, p. 24.

[14] I. Boldea, L. N. Tutelea, W. Xu, and M. Pucci, "Linear electric machines, drives, and MAGLEVs: An overview," *IEEE Transactions on Industrial Electronics*, vol. 65, no. 9, pp. 7504–7515, Sep. 2018. DOI: 10.1109/TIE.2017.2733492.

[15] B. Dalla Chiara, D. De Franco, N. Coviello, and D. Pastrone, "Comparative specific energy consumption between air transport and high-speed rail transport: A practical assessment," *Transportation Research Part D: Transport and Environment*, vol. 52, pp. 227–243, May 2017. DOI: 10.1016/j.trd.2017.02.006.

[16] J. K. Nøland, "Prospects and challenges of the hyperloop transportation system: A systematic technology review," *IEEE Access*, vol. 9, pp. 28 439–28 458, 2021. DOI: 10.1109/ACCESS.2021.3057788.

[17] G. McLean, "Review of recent progress in linear motors," *IEE Proceedings B Electric Power Applications*, vol. 135, no. 6, p. 380, 1988. DOI: 10.1049/ip-b.1988.0042.

[18] I. Boldea, *Linear Electric Machines, Drives, and MAGLEVs Handbook*. CRC Press ; Taylor & Francis, 2013, 652 pp.

[19] J. Gieras, Z. Piech, and B. Tomczuk, *Linear Synchronous Motors: Transportation and Automation Systems*, 2nd ed. Boca Raton: CRC Press, 2012, 534 pp.

[20] J. F. Gieras, *Linear induction drives* (Monographs in electrical and electronic engineering 30). Oxford : New York: Clarendon Press ; Oxford University Press, 1994, 298 pp.

[21] S. Yamamura, *Theory of linear induction motors*. New York: Wiley, 1972, 161 pp.

[22] E. R. Laithwaite, *Induction machines for special purposes*. London: George Newnes Ltd, 1966, 337 pp.

[23] I. Boldea, *Linear Motion Electromagnetic Devices*. New York, NY: Taylor & Francis, Nov. 5, 2001, 270 pp.

[24] I. Boldea and S. A. Nasar, *Linear electric actuators and generators*. Cambridge ; New York: Cambridge University Press, 1997, 237 pp.

[25] S. Yamamura, "Magnetic levitation technology of tracked vehicles present status and prospects," *IEEE Transactions on Magnetics*, vol. 12, no. 6, pp. 874–878, Nov. 1976. DOI: 10.1109/TMAG.1976.1059125.

[26] J. Pyrhonen, T. Jokinen, and V. Hrabovcová, *Design of rotating electrical machines*. Chichester, West Sussex, United Kingdom ; Hoboken, NJ: Wiley, 2008, 512 pp.

[27] A. Cassat and M. Jufer, "MAGLEV projects technology aspects and choices," *IEEE Transactions on Applied Superconductivity*, vol. 12, no. 1, pp. 915–925, Mar. 2002. DOI: 10.1109/TASC.2002.1018549.

[28] B. Kaiser and N. Parspour, "Transverse flux machine—a review," *IEEE Access*, vol. 10, pp. 18 395–18 419, 2022. DOI: 10.1109/ACCESS.2022.3150905.

[29] J. Eastham, M. Balchin, P. Coles, and D. Rodger, "Comparison of short primary linear machines for high speed maglev vehicles," *IEEE Transactions on Magnetics*, vol. 23, no. 5, pp. 2338–2343, Sep. 1987. DOI: 10.1109/TMAG.1987.1065313.

[30] E. R. Laithwaite and H. R. Bolton, "Linear motors with transverse flux," vol. 118, no. 12, 1971.

[31] S. Chevailler, "Comparative study and selection criteria of linear motors," Ph.D. dissertation, EPFL, Lausanne, May 22, 2006, 225 pp.

[32] J. Eastham, "Iron-cored linear synchronous machines," *Electronics and Power*, vol. 23, no. 3, pp. 239–242, Mar. 1977. DOI: 10.1049/ep.1977.0127.

[33] R. Palka and K. Woronowicz, "Linear induction motors in transportation systems," *Energies*, vol. 14, no. 9, p. 2549, Apr. 29, 2021. DOI: 10.3390/en14092549.

[34] M. H. Ravanji and Z. Nasiri-Gheidari, "Design optimization of a ladder secondary single-sided linear induction motor for improved performance," *IEEE Transactions on Energy Conversion*, vol. 30, no. 4, pp. 1595–1603, Dec. 2015. DOI: 10.1109/TEC.2015.2461434.

[35] D.-Y. Jeon, D. Kim, S.-Y. Hahn, and G. Cha, "Optimum design of linear synchronous motor using evolution strategy combined with stochastic FEM," *IEEE Transactions on Magnetics*, vol. 35, no. 3, pp. 1734–1737, May 1999. DOI: 10.1109/20.767364.

[36] S. Vaez-Zadeh and A. Isfahani, "Multiobjective design optimization of air-core linear permanent-magnet synchronous motors for improved thrust and low magnet consumption," *IEEE Transactions on Magnetics*, vol. 42, no. 3, pp. 446–452, Mar. 2006. DOI: 10.1109/TMAG.2005.863084.

[37] C. Lucas, Z. Nasiri-Gheidari, and F. Tootoonchian, "Application of an imperialist competitive algorithm to the design of a linear induction motor," *Energy Conversion and Management*, vol. 51, no. 7, pp. 1407–1411, Jul. 2010. DOI: 10.1016/j.enconman.2010.01.014.

[38] D. Hu, W. Xu, and R. Qu, "Electromagnetic design optimization of single-sided linear induction motor for improved drive performance based on linear metro application," in *2014 Australasian Universities Power Engineering Conference (AUPEC)*, Perth, Australia: IEEE, Sep. 2014, pp. 1–6. DOI: 10.1109/AUPEC.2014.6966564.

[39] A. A. Pourmoosa and M. Mirsalim, "Design optimization, prototyping, and performance evaluation of a low-speed linear induction motor with toroidal winding," *IEEE Transactions on Energy Conversion*, vol. 30, no. 4, pp. 1546–1555, Dec. 2015. DOI: 10.1109/TEC.2015.2457397.

[40] D. Hu, W. Xu, G. Lei, and J. Zhu, "Design and control optimization of linear induction motor drive for efficiency improvement," in *2017 20th International Conference on Electrical Machines and Systems (ICEMS)*, Sydney, Australia: IEEE, Aug. 2017, pp. 1–6. DOI: 10.1109/ICEMS.2017.8056320.

[41] A. Shiri and A. Tessarolo, "Normal force elimination in single-sided linear induction motor using design parameters," *IEEE Transactions on Transportation Electrification*, vol. 9, no. 1, pp. 394–403, Mar. 2023. DOI: 10.1109/TTE.2022.3183535.

[42] H. Wang, J. Zhao, G. Guo, H. Chen, Y. Xiong, and S. Yan, "Modeling and optimal design of a short primary double-sided linear induction motor considering both transverse and longitudinal end effects using improved differential evolution," *Journal of Electrical Engineering & Technology*, vol. 18, no. 2, pp. 1065–1081, Mar. 2023. DOI: 10.1007/s42835-022-01168-2.

[43] K. Wang, Y. Hu, Q. Wang, and Q. Ge, "Optimization of secondary iron of homopolar linear synchronous motor for traction application based on finite element method and regression model," in *2023 5th Asia Energy and Electrical Engineering Symposium (AEEES)*, Chengdu, China: IEEE, Mar. 23, 2023, pp. 453–459. DOI: 10.1109/AEEES56888.2023.10114261.

[44] W. Xu, X. Xiao, G. Du, D. Hu, and J. Zou, "Comprehensive efficiency optimization of linear induction motors for urban transit," *IEEE Transactions on Vehicular Technology*, vol. 69, no. 1, pp. 131–139, Jan. 2020. DOI: 10.1109/TVT.2019.2953956.

[45] J. Jiang, Q. Jiang, and S. Xiao, "Electromagnetic optimization of single-sided linear induction motors based on the genetic algorithm," in *2019 International Conference on Intelligent Computing, Automation and Systems (ICICAS)*, Chongqing, China: IEEE, Dec. 2019, pp. 329–334. DOI: 10.1109/ICICAS48597.2019.00077.

[46] A. Shiri and A. Shoulaie, "Design optimization and analysis of single-sided linear induction motor, considering all phenomena," *IEEE*

Transactions on Energy Conversion, vol. 27, no. 2, pp. 516–525, Jun. 2012. DOI: 10.1109/TEC.2012.2190416.

[47] A. Zare Bazghaleh, M. R. Naghashan, and M. R. Meshkatoddini, "Optimum design of single-sided linear induction motors for improved motor performance," *IEEE Transactions on Magnetics*, vol. 46, no. 11, pp. 3939–3947, Nov. 2010. DOI: 10.1109/TMAG.2010.2062528.

[48] A. H. Isfahani, B. M. Ebrahimi, and H. Lesani, "Design optimization of a low-speed single-sided linear induction motor for improved efficiency and power factor," *IEEE Transactions on Magnetics*, vol. 44, no. 2, pp. 266–272, Feb. 2008. DOI: 10.1109/TMAG.2007.912646.

[49] G. Slemon, R. Turton, and P. Burke, "A linear synchronous motor for high-speed ground transport," *IEEE Transactions on Magnetics*, vol. 10, no. 3, pp. 435–438, Sep. 1974. DOI: 10.1109/TMAG.1974.1058453.

[50] S.-B. Yoon, J. Hur, and D.-S. Hyun, "A method of optimal design of single-sided linear induction motor for transit," *IEEE Transactions on Magnetics*, vol. 33, no. 5, pp. 4215–4217, Sep. 1997. DOI: 10.1109/20.619714.

[51] T. A. Nondahl, "Design studies for single-sided linear electric motors: Homopolar synchronous and induction," *Electric Machines & Power Systems*, vol. 5, no. 1, pp. 1–14, Jan. 1980. DOI: 10.1080/07313568008955386.

[52] Z. Zhao, K. Liu, C. Wang, *et al.*, "The establishment of an analytical model for coreless HTS linear synchronous motor with a generalized racetrack coil as the secondary," *IEEE Transactions on Applied Superconductivity*, vol. 29, no. 5, pp. 1–5, Aug. 2019. DOI: 10.1109/TASC.2019.2901015.

[53] L. Shi, Z. Yin, L. Jiang, and Y. Li, "Advances in inductively coupled power transfer technology for rail transit," *CES Transactions on Electrical Machines and Systems*, vol. 1, no. 4, pp. 383–396, Dec. 2017. DOI: 10.23919/TEMS.2017.8241360.

[54] B.-J. Lee, D.-H. Koo, and Y.-H. Cho, "Investigation of linear induction motor according to secondary conductor structure," *IEEE Transactions on Magnetics*, vol. 45, no. 6, pp. 2839–2842, Jun. 2009. DOI: 10.1109/TMAG.2009.2018687.

[55] G. E. Dawson and T. R. Eastham, "The comparative performance of single-sided linear induction motors with squirrel-cage, solid-steel and aluminum-capped reaction rails," in *1981 Annual Meeting Industry Applications Society*, 1981, pp. 323–329.

[56] D. Tsang. "SkyTrain OMC tour." (Oct. 2019), [Online]. Available: https://dennistt.net/2019/10/04/skytrain-omc-tour/.

[57] A. Meskens. "The AirTrain JFK a people mover at john f. kennedy international airport.," Wikimedia Commons. (Apr. 14, 2012), [Online]. Available: https://commons.wikimedia.org/wiki/File:JFK_AirTrain_02.JPG.

[58] J. F. Gieras, A. R. Eastham, and G. E. Dawson, "Performance calculation for single-sided linear induction motors with a solid steel reaction plate under constant current excitation," *IEE Proceedings B (Electric Power Applications)*, vol. 132, no. 4, pp. 185–194, Jul. 1, 1985. DOI: 10.1049/ip-b.1985.0027.

[59] R. J. A. Bevan, "An experimental evaluation of a full-scale single-sided linear induction motor with difference reaction rails. volume i: Test results," Dec. 1981.

[60] M. Iwamoto, S. Sakabe, K. Kitagawa, and G. Utsumi, "Experimental and theoretical study of high-speed single-sided linear induction motors," *IEE Proceedings B Electric Power Applications*, vol. 128, no. 6, p. 306, 1981. DOI: 10.1049/ip-b.1981.0054.

[61] A. Eastham and R. Katz, "The operation of a single-sided linear induction motor with squirrel-cage and solid-steel reaction rails," *IEEE Transactions on Magnetics*, vol. 16, no. 5, pp. 722–724, Sep. 1980. DOI: 10.1109/TMAG.1980.1060722.

[62] S. Nasar and L. Del Cid, "Propulsion and levitation forces in a single-sided linear induction motor for high-speed ground transportation," *Proceedings of the IEEE*, vol. 61, no. 5, pp. 638–644, May 1973. DOI: 10.1109/PROC.1973.9121.

[63] B. I. Kwon, K. I. Woo, S. Kim, and S. C. Park, "Analysis for dynamic characteristics of a single-sided linear induction motor having joints in the secondary conductor and back-iron," *IEEE Transactions on Magnetics*, vol. 36, no. 4, pp. 823–826, Jul. 2000. DOI: 10.1109/20.877571.

[64] Q. Lu, L. Li, J. Zhan, X. Huang, and J. Cai, "Design optimization and performance investigation of novel linear induction motors with two kinds of secondaries," *IEEE Transactions on Industry Applications*, vol. 55, no. 6, pp. 5830–5842, Nov. 2019. DOI: 10.1109/TIA.2019.2937857.

[65] M. Iwamoto, E. Ohno, T. Itoh, and Y. Shinryo, "End-effect of high-speed linear induction motor," *IEEE Transactions on Industry Applications*, vol. IA-9, no. 6, pp. 632–639, Nov. 1973, Conference Name: IEEE Transactions on Industry Applications. DOI: 10.1109/TIA.1973.349986.

[66] T. C. Wang, "Linear induction motor for high-speed ground transportation," *IEEE Transactions on Industry and General Applications*, vol. IGA-7, no. 5, pp. 632–642, Sep. 1971. DOI: 10.1109/TIGA.1971.4181356.

[67] T. Higuchi, S. Nonaka, and M. Ando, "On the design of high-efficiency linear induction motors for linear metro," *Electrical Engineering in Japan*, vol. 137, no. 2, pp. 36–43, Nov. 15, 2001. DOI: 10.1002/eej.1086.

[68] G. Lv, D. Zeng, T. Zhou, and Z. Liu, "Investigation of forces and secondary losses in linear induction motor with the solid and laminated back iron secondary for metro," *IEEE Transactions on Industrial Electronics*, vol. 64, no. 6, pp. 4382–4390, Jun. 2017. DOI: 10.1109/TIE.2016.2565442.

[69] R. C. Creppe, J. A. C. Ulson, and J. F. Rodrigues, "Influence of design parameters on linear induction motor end effect," *IEEE Transactions on Energy Conversion*, vol. 23, no. 2, pp. 358–362, Jun. 2008. DOI: 10.1109/TEC.2008.918594.

[70] J. F. Gieras, G. E. Dawson, and A. R. Eastham, "A new longitudinal end effect factor for linear induction motors," *IEEE Transactions on Energy Conversion*, vol. EC-2, no. 1, pp. 152–159, Mar. 1987. DOI: 10.1109/TEC.1987.4765816.

[71] E. Laithwaite and S. Kuznetsov, "Power-factor improvement in linear induction motors," *IEE Proceedings B Electric Power Applications*, vol. 128, no. 4, p. 190, 1981. DOI: 10.1049/ip-b.1981.0030.

[72] S. Yamamura, H. Ito, and Y. Ishulawa, "Theories of the linear, induction motor and compensated linear induction motor," *IEEE Transactions on Power Apparatus and Systems*, vol. PAS-91, no. 4, pp. 1700–1710, Jul. 1972. DOI: 10.1109/TPAS.1972.293349.

[73] D. Zeng, G. Lv, and T. Zhou, "Equivalent circuits for single-sided linear induction motors with asymmetric cap secondary for linear transit," *IEEE Transactions on Energy Conversion*, vol. 33, no. 4, pp. 1729–1738, Dec. 2018. DOI: 10.1109/TEC.2018.2840057.

[74] G. Lv, D. Zeng, and T. Zhou, "An advanced equivalent circuit model for linear induction motors," *IEEE Transactions on Industrial Electronics*, vol. 65, no. 9, pp. 7495–7503, Sep. 2018. DOI: 10.1109/TIE.2018.2807366.

[75] K. Woronowicz and A. Safaee, "A novel linear induction motor equivalent-circuit with optimized end effect model," *Canadian Journal of Electrical and Computer Engineering*, vol. 37, no. 1, pp. 34–41, 2014, Conference Name: Canadian Journal of Electrical and Computer Engineering. DOI: 10.1109/CJECE.2014.2311958.

[76] K. Woronowicz and A. Safaee, "Linear motor drives and applications in rapid transit systems," in *2014 IEEE Transportation Electrification Conference and Expo (ITEC)*, Jun. 2014, pp. 1–96. DOI: 10.1109/ITEC.2014.6861817.

[77] W.-Y. Ji, G. Jeong, C.-B. Park, I.-H. Jo, and H.-W. Lee, "A study of non-symmetric double-sided linear induction motor for hyperloop all-in-one system (propulsion, levitation, and guidance)," *IEEE Transactions on Magnetics*, vol. 54, no. 11, pp. 1–4, Nov. 2018. DOI: 10.1109/TMAG.2018.2848292.

[78] M. S. Hosseini and S. Vaez-Zadeh, "Modeling and analysis of linear synchronous motors in high-speed maglev vehicles," *IEEE Transactions on Magnetics*, vol. 46, no. 7, pp. 2656–2664, Jul. 2010. DOI: 10.1109/TMAG.2009.2039999.

[79] F. Carter, "The magnetic field of the dynamo-electric machine," *Journal of the Institution of Electrical Engineers*, vol. 64, no. 359, pp. 1115–1138, Nov. 1926. DOI: 10.1049/jiee-1.1926.0122.

[80] J. Duncan, "Linear induction motor-equivalent-circuit model," *IEE Proceedings B Electric Power Applications*, vol. 130, no. 1, p. 51, 1983. DOI: 10.1049/ip-b.1983.0008.

[81] K. Woronowicz, M. Abdelqader, R. Palka, and J. Morelli, "2-d quasi-static fourier series solution for a linear induction motor," *COMPEL - The international journal for computation and mathematics in electrical and electronic engineering*, vol. 37, no. 3, pp. 1099–1109, Jan. 1, 2018, Publisher: Emerald Publishing Limited. DOI: 10.1108/COMPEL-06-2017-0247.

[82] G. Lv, T. Zhou, D. Zeng, and Z. Liu, "Design of ladder-slit secondaries and performance improvement of linear induction motors for urban rail transit," *IEEE Transactions on Industrial Electronics*, vol. 65, no. 2, pp. 1187–1195, Feb. 2018. DOI: 10.1109/TIE.2017.2726967.

[83] S. Rametti, L. Pierrejean, A. Hodder, and M. Paolone, "Pseudo-three-dimensional analytical model of linear induction motors for high-speed applications," *IEEE Transactions on Transportation Electrification*, pp. 1–1, 2024. DOI: 10.1109/TTE.2023.3348655.

[84] I. Boldea and S. A. Nasar, *The induction machines design handbook* (The electric power engineering series), 2nd ed. Boca Raton, FL: CRC Press ; Taylor & Francis, 2010, 827 pp.

[85] S. Nonaka and T. Higuchi, "Design of single-sided linear induction motors for urban transit," *IEEE Transactions on Vehicular Technology*, vol. 37, no. 3, pp. 167–173, Aug. 1988. DOI: 10.1109/25.16543.

[86] O. Coho, G. Kliman, and J. Robinson, "Experimental evaluation of a high speed double sided linear induction motor," *IEEE Transactions on Power Apparatus and Systems*, vol. 94, no. 1, pp. 10–17, Jan. 1975. DOI: 10.1109/T-PAS.1975.31818.

[87] O. Hibi and K. Saito, "Summary of automatic operation of linimo and achievement in opening year," presented at the The 19th International Conference on Magnetically Levitated Systems and Linear Drives, Sep. 13, 2006.

[88] H.-S. Han and D.-S. Kim, *Magnetic Levitation* (Springer Tracts on Transportation and Traffic). Dordrecht: Springer Netherlands, 2016, vol. 13.

[89] G. Lv, L. Cui, R. Zhi, T. Zhou, and Y. Liu, "Investigation of the transverse flux linear synchronous motor integrated with propulsion, levitation and guidance for the maglev train," *IEEE Transactions on Transportation Electrification*, pp. 1–1, 2023. DOI: 10.1109/TTE.2023.3246070.

[90] G. Bohn and G. Steinmetz, "The electromagnetic levitation and guidance technology of the 'transrapid' test facility emsland," *IEEE Transactions on Magnetics*, vol. 20, no. 5, pp. 1666–1671, Sep. 1984. DOI: 10.1109/TMAG.1984.1063246.

[91] Jklamo. "Shanghai maglev train line with approaching transrapid 08 SMT," Wikimedia Commons. (Mar. 26, 2014), [Online]. Available: https://commons.wikimedia.org/wiki/File:ShanghaiMaglevTrainLine_06.jpg.

[92] M. A. Rosenmayr, "Swissmetro: Speisung und Regelung des Linearantriebs," Ph.D. dissertation, ETH Zurich, 2000.

[93] I. Boldea, A. Trica, G. Papusoiu, and S. Nasar, "Field tests on a MAGLEV with passive guideway linear inductor motor transportation system," *IEEE Transactions on Vehicular Technology*, vol. 37, no. 4, pp. 213–219, Nov. 1988. DOI: 10.1109/25.31126.

[94] N. Prasad, S. Jain, and S. Gupta, "Review of linear switched reluctance motor designs for linear propulsion applications," *CES Transactions on Electrical Machines and Systems*, vol. 6, no. 2, pp. 179–187, Jun. 2022. DOI: 10.30941/CESTEMS.2022.00024.

[95] X. Xiao, W. Xu, X. Li, *et al.*, "Novel homopolar linear synchronous motor with e-shape primary core," in *2018 21st International Conference on Electrical Machines and Systems (ICEMS)*, Oct. 2018, pp. 1821–1826. DOI: 10.23919/ICEMS.2018.8549164.

[96] I. Boldea and S. A. Nasar, "Linear synchronous homopolar motor (LSHM)—a design procedure for propulsion and levitation system," *Electric Machines & Power Systems*, vol. 4, no. 2, pp. 125–135, Sep. 1979. DOI: 10.1080/07313567908955366.

[97] R. Cao, E. Su, M. Lu, J. Si, and K. Wang, "Investigation of linear synchronous reluctance motor for urban rail transit," *IET Electric Power Applications*, vol. 14, no. 1, pp. 41–51, 2020. DOI: 10.1049/iet-epa.2019.0410.

[98] I. Boldea and S. A. Nasar, "Thrust and normal forces in a segmented-secondary linear reluctance motor," *Proceedings of the Institution of Electrical Engineers*, vol. 122, no. 9, pp. 922–924, Sep. 1, 1975. DOI: 10.1049/piee.1975.0249.

[99] I. Boldea, *Reluctance synchronous machines and drives* (Monographs in electrical and electronic engineering 38). Oxford, England : New York: Clarendon Press ; Oxford University Press, 1996, 230 pp.

[100] R. Cao, M. Lu, N. Jiang, and M. Cheng, "Comparison between linear induction motor and linear flux-switching permanent-magnet motor for railway transportation," *IEEE Transactions on Industrial Electronics*, vol. 66, no. 12, pp. 9394–9405, Dec. 2019. DOI: 10.1109/TIE.2019.2892676.

[101] H. Weh and M. Shalaby, "Magnetic levitation with controlled permanentic excitation," *IEEE Transactions on Magnetics*, vol. 13, no. 5, pp. 1409–1411, Sep. 1977. DOI: 10.1109/TMAG.1977.1059567.

[102] D. Atherton and S. Fraser, "A homopolar linear synchronous test motor using permanent magnets," *IEEE Transactions on Magnetics*, vol. 18, no. 6, pp. 1843–1846, Nov. 1982, Conference Name: IEEE Transactions on Magnetics. DOI: 10.1109/TMAG.1982.1062050.

[103] T. Murai, T. Fujimoto, and S. Fujirawa, "Test run of combined propulsion, levitation and guidance system in EDS maglev," presented at the MAGLEV '95 14th Int. Conf. on Magnetically Levitated Systems, Bremen, Germany, Nov. 1995.

[104] C. J. R. Company. "Superconducting maglev gallery." (), [Online]. Available: https://scmaglev.jr-central-global.com/gallery/.

[105] D. Atherton, A. Eastham, J. Cunningham, S. Dewan, G. Slemon, and R. Turton, "Design, analysis and test results for a superconducting linear synchronous motor," *Proceedings of the Institution of Electrical Engineers*, vol. 124, no. 4, p. 363, 1977. DOI: 10.1049/piee.1977.0066.

[106] G. Lv, Z. Zhang, and X. Li, "Three-dimensional electromagnetic characteristics analysis of novel linear synchronous motor under lateral and yaw conditions of MAGLEV," *CES Transactions on Electrical Machines and Systems*, vol. 6, no. 1, pp. 29–36, Mar. 2022. DOI: 10.30941/CESTEMS.2022.00005.

[107] Z. Zhao, G. Ma, K. Liu, *et al.*, "3-d analysis of electromagnetic forces of a real-scale superconducting linear synchronous motor for EDS train," *IEEE Transactions on Applied Superconductivity*, vol. 31, no. 5, pp. 1–5, Aug. 2021. DOI: 10.1109/TASC.2021.3059390.

[108] I. Boldea and S. A. Nasar, *Linear motion electromagnetic systems*. New York: Wiley, 1985, 482 pp.

[109] W. R. Mischler and T. Nondahl, "Performance of a linear synchronous motor with laminated track poles and with various misalignments," FRA/ORD-80/52-1, Sep. 1980.

[110] I. Boldea and S. A. Nasar, "Field winding drag and normal forces of linear synchronous homopolar motors," *Electric Machines & Power Systems*, vol. 2, no. 3, pp. 253–268, Apr. 1, 1978. DOI: 10.1080/03616967808955309.

[111] J. Eastham, M. Balchin, and P. Coles, "Full-scale testing of a high speed linear synchronous motor and calculation of end-effects," *IEEE Transactions on Magnetics*, vol. 24, no. 6, pp. 2892–2894, Nov. 1988. DOI: 10.1109/20.92279.

[112] G. R. Slemon and R. P. Bhatia, "Linear homopolar synchronous motor for urban transit application," *Canadian Electrical Engineering Journal*, vol. 7, no. 2, pp. 12–20, Apr. 1982. DOI: 10.1109/CEEJ.1982.6594618.

[113] H. Lorenzen, R. Nuscheler, and A. Meyer, "Experimental investigation of the operating behaviour of linear synchronous motors," *IEEE Transactions on Energy Conversion*, vol. EC-1, no. 4, pp. 73–82, Dec. 1986, Conference Name: IEEE Transactions on Energy Conversion. DOI: 10.1109/TEC.1986.4765778.

[114] D. Atherton, "A magnetic circuit analysis of the iron-cored homopolar linear synchronous motor," *IEEE Transactions on Magnetics*, vol. 17, no. 3, pp. 1305–1310, May 1981, Conference Name: IEEE Transactions on Magnetics. DOI: 10.1109/TMAG.1981.1061204.

[115] G. Lv, Y. Liu, Z. Zhang, and T. Zhou, "Characteristic analysis of coreless-type linear synchronous motor with the racetrack coils as secondary for EDS maglev train," *IEEE/ASME Transactions on Mechatronics*, vol. 27, no. 6, pp. 4654–4664, Dec. 2022, Conference Name: IEEE/ASME Transactions on Mechatronics. DOI: 10.1109/TMECH.2022.3163520.

[116] G. Lv, Z. Zhang, Y. Liu, and T. Zhou, "Analysis of forces in linear synchronous motor with propulsion, levitation and guidance for high-speed maglev," *IEEE Journal of Emerging and Selected Topics in Power Electronics*, vol. 10, no. 3, pp. 2903–2911, Jun. 2022, Conference Name: IEEE Journal of Emerging and Selected Topics in Power Electronics. DOI: 10.1109/JESTPE.2021.3065459.

[117] G. Lv, L. Cui, and R. Zhi, "Inductance analysis of transverse flux linear synchronous motor for maglev trains considering three-dimensional operating conditions," *IEEE Transactions on Industrial Electronics*, vol. 71, no. 1, pp. 769–776, Jan. 2024. DOI: 10.1109/TIE.2023.3250754.

[118] X. Xiao, W. Xu, D. Luo, and I. Boldea, "Improved 2d FEA model for homopolar linear synchronous machine," in *2020 IEEE 9th International Power Electronics and Motion Control Conference (IPEMC2020-ECCE Asia)*, Nov. 2020, pp. 3410–3414. DOI: 10.1109/IPEMC-ECCEAsia48364.2020.9368174.

[119] S. Al-Kasimi, "A new linear synchronous motor for mag-lev train with integrated lift and thrust using a trapezoidal rail," in *[1992 Proceedings] Vehicular Technology Society 42nd VTS Conference - Frontiers of Technology*, May 1992, 209–212 vol.1. DOI: 10.1109/VETEC.1992.245439.

[120] G. McLean and A. West, "Combined lift and thrust for maglev vehicles using the zig-zag synchronous motor," in *I Mech E Conference Publications (Institution of Mechanical Engineers)*, 1984, pp. 87–93.

[121] Z. Zhu and D. Howe, "Instantaneous magnetic field distribution in brushless permanent magnet DC motors. III. effect of stator slotting,"

IEEE Transactions on Magnetics, vol. 29, no. 1, pp. 143–151, Jan. 1993. DOI: 10.1109/20.195559.

[122] D. Zarko, D. Ban, and T. Lipo, "Analytical calculation of magnetic field distribution in the slotted air gap of a surface permanent-magnet motor using complex relative air-gap permeance," *IEEE Transactions on Magnetics*, vol. 42, no. 7, pp. 1828–1837, Jul. 2006. DOI: 10.1109/TMAG.2006.874594.

[123] M. Wang, J. Zhu, L. Guo, J. Wu, and Y. Shen, "Analytical calculation of complex relative permeance function and magnetic field in slotted permanent magnet synchronous machines," *IEEE Transactions on Magnetics*, vol. 57, no. 3, pp. 1–9, Mar. 2021. DOI: 10.1109/TMAG.2020.3046354.

[124] D. H. Kang and H. Weh, "Design of an integrated propulsion, guidance, and levitation system by magnetically excited transverse flux linear motor (TFM-LM)," *IEEE Transactions on Energy Conversion*, vol. 19, no. 3, pp. 477–484, Sep. 2004, Conference Name: IEEE Transactions on Energy Conversion. DOI: 10.1109/TEC.2004.832051.

[125] B. Sheikh-Ghalavand, S. Vaez-Zadeh, and A. Hassanpour Isfahani, "An improved magnetic equivalent circuit model for iron-core linear permanent-magnet synchronous motors," *IEEE Transactions on Magnetics*, vol. 46, no. 1, pp. 112–120, Jan. 2010. DOI: 10.1109/TMAG.2009.2030674.

[126] Q. Lu, B. Wu, Y. Yao, Y. Shen, and Q. Jiang, "Analytical model of permanent magnet linear synchronous machines considering end effect and slotting effect," *IEEE Transactions on Energy Conversion*, vol. 35, no. 1, pp. 139–148, Mar. 2020. DOI: 10.1109/TEC.2019.2946278.

[127] D. Krop, E. Lomonova, and A. Vandenput, "Application of schwarz-christoffel mapping to permanent-magnet linear motor analysis," *IEEE Transactions on Magnetics*, vol. 44, no. 3, pp. 352–359, Mar. 2008. DOI: 10.1109/TMAG.2007.914513.

[128] Shi-Uk Chung, Hong-Joo Lee, and Sang-Moon Hwang, "A novel design of linear synchronous motor using FRM topology," *IEEE Transactions on Magnetics*, vol. 44, no. 6, pp. 1514–1517, Jun. 2008. DOI: 10.1109/TMAG.2007.915104.

[129] R. G. Gilliland and G. W. Pearson, "A linear synchronous unipolar motor for integrated magnetic propulsion and suspension," in *Proc. of Int. Conf. on MAGLEV*, Vancouver, Canada: Institute of electrical and electronic engineers, May 1986, pp. 149–155.

[130] G. Dawson, A. Eastham, and R. Ong, "Computer-aided design studies of the homopolar linear synchronous motor," *IEEE Transactions on Magnetics*, vol. 20, no. 5, pp. 1927–1929, Sep. 1984. DOI: 10.1109/TMAG.1984.1063452.

[131] A. Farhadi, H. Yousefi, Y. Noorollahi, and A. Hajinezhad, "A comprehensive analysis on a novel DC-excited flux-switching linear motor as a new linear vehicle for transportation systems," *IET Electric Power Applications*, vol. 17, no. 1, pp. 36–46, 2023. DOI: 10.1049/elp2.12243.

[132] F. Rüdiger, "Design elements and quantitative results of synchronous long-stator linear motor for high-speed magnetic trains taking the transrapid test facility in emsland as an example," presented at the MAGLEV '95 14th Int. Conf. on Magnetically Levitated Systems, Bremen, Germany, Nov. 1995.

[133] H.-W. Cho, H.-K. Sung, S.-Y. Sung, D.-J. You, and S.-M. Jang, "Design and characteristic analysis on the short-stator linear synchronous motor for high-speed maglev propulsion," *IEEE Transactions on Magnetics*, vol. 44, no. 11, pp. 4369–4372, Nov. 2008, Conference Name: IEEE Transactions on Magnetics. DOI: 10.1109/TMAG.2008.2001511.

[134] M. Andriollo, G. Martinelli, A. Morini, and A. Tortella, "FEM calculation of the LSM propulsion force in EMS-MAGLEV trains," *IEEE Transactions on Magnetics*, vol. 32, no. 5, pp. 5064–5066, Sep. 1996. DOI: 10.1109/20.539491.

[135] T. Murai, "Characteristics of LSM combined propulsion, levitation and guidance," *Electrical Engineering in Japan*, vol. 115, no. 4, pp. 134–145, Jun. 15, 1995. DOI: 10.1002/eej.4391150412.

[136] Z. Zhao, G. Ma, J. Luo, J. Li, Z. Su, and K. Liu, "Modeling and characteristic analysis of air-cored linear synchronous motors with racetrack coils for electrodynamic suspension train," *IEEE Transactions on Transportation Electrification*, vol. 8, no. 2, pp. 1828–1838, Jun. 2022. DOI: 10.1109/TTE.2021.3126595.

[137] E. Ohno, M. Iwamoto, and T. Yamada, "Characteristics of superconductive magnetic suspension and propulsion for high-speed trains," *Proceedings of the IEEE*, vol. 61, no. 5, pp. 579–586, May 1973. DOI: 10.1109/PROC.1973.9114.

[138] D. Atherton, "Desgin and control studies of a linear synchronous motor for urban transit application," *IEEE Transactions on Magnetics*, vol. 18, no. 6, pp. 1847–1855, Nov. 1982. DOI: 10.1109/TMAG.1982.1062024.

[139] S. Y. Choi, C. Y. Lee, J. M. Jo, *et al.*, "Sub-sonic linear synchronous motors using superconducting magnets for the hyperloop," *Energies*, vol. 12, no. 24, p. 4611, Dec. 4, 2019. DOI: 10.3390/en12244611.

[140] E. Levi, "Linear synchronous motors for high-speed ground transportation," *IEEE Transactions on Magnetics*, vol. 9, no. 3, pp. 242–248, Sep. 1973. DOI: 10.1109/TMAG.1973.1067639.

[141] M. J. Balchin, J. F. Eastham, and P. C. Coles, "Effects of pole flux distribution in a homopolar linear synchronous machine," *Journal of Applied Physics*, vol. 75, no. 10, pp. 6987–6989, May 15, 1994. DOI: 10.1063/1.356750.

[142] I. Boldea, "Magnibus - the romanian linear inductor (synchronous) motor (passive guideway) maglev," in *I Mech E Conference Publications (Institution of Mechanical Engineers)*, 1984, pp. 149–154.

[143] A. Cassat and C. Espanet, "SWISSMETRO: Combined propulsion with levitation and guidance," presented at the MAGLEV 2004, vol. 2, Shanghai, China: Proceedings of MAGLEV 2004, Aug. 26, 2004, pp. 747–758.

[144] J. He, D. Rote, and H. Coffey, "Survey of foreign maglev systems," Argonne National Lab,Energy Systems Div., IL, U.S., Technical ANL/ESD-17, Jul. 1992.

[145] R. Pai, I. Boldea, and S. Nasar, "A complete equivalent circuit of a linear induction motor with sheet secondary," *IEEE Transactions on Magnetics*, vol. 24, no. 1, pp. 639–654, Jan. 1988. DOI: 10.1109/20.43997.

[146] J. Colmery, R. Day, G. Kalman, and S. Mitchell, "Design and testing of a 12,000 KVA linear induction motor and power converter," Torrance, US, FRA/ORD-76/305, Jun. 1977, p. 327.

[147] S. Suzuki, M. Kawashima, Y. Hosoda, and T. Tanida, "HSST-03 system," *IEEE Transactions on Magnetics*, vol. 20, no. 5, pp. 1675–1677, Sep. 1984, Conference Name: IEEE Transactions on Magnetics. DOI: 10.1109/TMAG.1984.1063210.

[148] Y. Nozaki and T. Koseki, "Identification of plant model of linear induction motors for a traction system intended for use in a high-performance controller," *Electrical Engineering in Japan*, vol. 179, no. 2, pp. 44–54, Apr. 30, 2012. DOI: 10.1002/eej.21171.

[149] S. Nakamura, Y. Takeuchi, and M. Takahashi, "Experimental results of the single- sided linear induction motor," *IEEE Transactions on Magnetics*, vol. 15, no. 6, pp. 1434–1436, Nov. 1979, Conference Name: IEEE Transactions on Magnetics. DOI: 10.1109/TMAG.1979.1060436.

[150] T. Lipa and T. Nondahl, "Pole-by-pole d-q model of a linear induction machine," *IEEE Transactions on Power Apparatus and Systems*, vol. PAS-98, no. 2, pp. 629–642, Mar. 1979. DOI: 10.1109/TPAS.1979.319448.

[151] N. D. Fintescu and J. P. Pascal, "Test results of full-scale 1mw linear induction motor ("u-LIM-AS") with PWM inverter," in *Proc. of Int. Conf. on MAGLEV*, Vancouver, Canada: Institute of electrical and electronic engineers, May 1986, pp. 165–170.

[152] G. R. Slemon, "An experimental study of a homopolar linear synchronous motor," *Electric Machines & Power Systems*, vol. 4, no. 1, pp. 59–70, Jul. 1979. DOI: 10.1080/07313567908955360.

[153] M. A. Rosenmayr, A. Cassat, H. Stemmler, and H. Glavitsch, "Swissmetro - power supply for a high-power propulsion system with short stator linear motors," presented at the Internation Conference on MAGLEV'98, Mount Fuji, Yamanashi, Japan, Apr. 1998.

[154] A. Cassat, N. Mababrey, and M. Jufer, "Swissmetro : tronçon pilote Genève - Lausanne : aspects électromécanique," 1998. DOI: 10.5169/SEALS-902088.

[155] K. Heinrich and R. Kretzschmar, Eds., *Transrapid MagLev system*, Darmstadt: Hestra-Verl, 1989, 113 pp.

[156] R. Friedrich, K. Dreimann, and R. Leistikow, "The power supply and the propulsion system of the transrapid 06 vehicle results of trials," in *Proc. of Int. Conf. on MAGLEV*, Vancouver, Canada: Institute of electrical and electronic engineers, May 1986, pp. 243–249.

[157] S. Abe, "Linear shinkansen as energy problem," *National Institute of Advanced Industrial Science and Technology*, vol. 83, no. 11, pp. 1290–1298, 2013.

[158] T. Saijo, S. Koike, and S. Tadakuma, "Characteristics of linear synchronous motor drive cycloconverter for maglev vehicle ML-500 at miyazaki test track," *IEEE Transactions on Industry Applications*, vol. IA-17, no. 5, pp. 533–543, Sep. 1981, Conference Name: IEEE Transactions on Industry Applications. DOI: 10.1109/TIA.1981.4503994.